# Sol phase and sol–gel transition in $SnO_2$ colloidal suspensions

**Léo Ricardo Bedore dos Santos [a], Aldo Felix Craievich [b], Celso Valentim Santilli [a] and Sandra Helena Pulcinelli [a]**

[a]*Institute of Chemistry, UNESP P.O. Box 355 14800-970 Araraquara, SP, Brazil*
[b]*Institute od Physics, USP, P.O. Box 66318 05315-970 São Paulo, SP, Brazil*
*Email:leosanto@iq.unesp.br*

The effect of concentration on the structure of $SnO_2$ colloids in aqueous suspension, on their spatial correlation and on the gelation process was studied by small angle x-ray scattering (SAXS). The shape of the experimental SAXS curves varies with suspension concentration. For diluted suspensions ($[SnO_2] \leq 0.13$ mol $L^{-1}$), SAXS results indicate the presence of colloidal fractal aggregates with an internal correlation length $\xi \cong 20$ Å, without any noticeable spatial correlation between them. This suggests that the aggregates are spatially arranged without any significant interaction like in ideal gas structures. For higher concentrations ($[SnO_2]$ = 0.16, 0.32, and 0.64 mol $L^{-1}$), the colloidal aggregates are larger ($\xi$ = 24 Å) and exhibit a certain degree of spatial correlation between them. The pair correlation function corresponding to the sol with the highest concentration (0.92 mol $L^{-1}$) reveals a rather strong short range order between aggregates, characteristic of a fluid-like structure, with an average nearest-neighbor distance between aggregates $d_1$ = 125 Å and an average second-neighbor distance $d_2$ = 283 Å. The pair distribution function remains essentially invariant during the sol-gel transition, suggesting that gelation involves the formation of a few points of connection between the aggregates resulting in a gel network constituted by essentially linear chains of clusters..

## 1. Introduction

The attention of materials scientists in ceramic membrane technology is growing very fast mainly due to interesting properties of these materials such as thermal, microbiological and mechanical resistance (Alami-Younssi et al, 1994). Among the inorganic oxides used for nano and ultrafiltration membrane preparation, $SnO_2$ exhibits interesting microstructural characteristics (Brito, Pulcinelli & Santilli, 1994; Santos, Pulcinelli & Santilli, 1997), such as the so-called dynamical scaling property for pore growth and sintering (Santilli, Pulcinelli & Craievich, 1995). This self-similar growth permits the preparation of membranes with different cut-off values without changing significantly the flux of the permeate (Santos et al., 1998).

Besides, the sol-gel process is a very versatile way for obtaining these membranes. In this process, the colloidal sols can be prepared, either by polycondensation of metal salts in aqueous solution or by hydrolysis and polycondensation reactions of metal alkoxides (Brinker & Scherrer, 1990; Cot, 1991). Indeed, a detailed knowledge of the structure of colloidal aggregates and of sol-gel transition is primordial to develop procedures to obtain crack-free membranes.

In a previous study of $SnO_2$ colloids (Briois et al., 1995) it was shown by spectroscopic measurements, that the primary particles are formed by nanocrystallites ( $\approx$ 8 Å) of cassiterite structure. During gelation, a secondary polycondensation reaction between superficial hydroxyl groups was observed (Hiratsuka, Pulcinelli & Santilli, 1990). Meanwhile, the nanostructural features of these aqueous colloidal systems are still unknown. Using the small-angle X-ray scattering (SAXS) technique, information concerning the structure of colloidal particles, the aggregation process and the formation of gel networks can be obtained (Vollet et al., 1992).

In this paper, we report a SAXS investigation of $SnO_2$ aqueous suspensions, focussing the effect of sol concentration on (i) the nanostructure of $SnO_2$ colloidal aggregates, (ii) the spatial correlation between them and (iii) the nature of the sol-gel transition.

## 2. Form factor and structure function for a concentrated set of fractal objects

The scattering power, $I(q)$, produced by an isotropic system composed of a homogeneous matrix in which randomly oriented and identical objects are embedded, is given by (Guinier, 1963):

$$I(q) = \phi P(q) S(q), \tag{1}$$

where $\phi$ is the number of colloidal objects per unit volume, $P(q)$ is the form factor of the colloidal objects and $S(q)$ is the structure function which accounts for the spatial correlation between them, and $q$ is defined by $q=(4\pi \sin \theta)/\lambda$, $\theta$ is half the scattering angle and $\lambda$ is the wavelength.

We have assumed that the $SnO_2$ colloidal aggregates embedded in the aqueous solvent are fractal objects. We will justify this assumption later. In order to determine the inter-aggregate structure function $S(q)$ from the experimental intensity curve, $I(q)$, the function defining the form factor $P(q)$ associated to an isolated colloidal aggregate must be known (equation 1).

The form factor $P(q)$ of an aggregate composed of small primary particles or monomers is given by

$$P(q)=I_1(q)= \varphi P'(q) S'(q), \tag{2}$$

where $\varphi$ is the number of monomers or primary particles that build up the aggregates, $P'(q)$ is the form factor of the primary particles and $S'(q)$ the intra-aggregate structure function associated to the spatial correlation between primary particles. Assuming that the aggregates have a fractal structure characterized by a correlation length $\xi$ and a primary particle size $a$, the intra-aggregate structure function $S'(q)$ can be written as (Teixeira, 1988)

$$S'(q) = (1+\{[1/(q\cdot a)^D]\times\{[D\cdot\Gamma(D-1)]/[1+(1/q^2\cdot\xi^2)]^{(D-1)/2}\}\times \sin[(D-1)\tan^{-1}(q\cdot\xi)]\}) \tag{3}$$

where $D$ is the dimensionality of the fractal aggregate and $\Gamma$ is the gamma function. This expression becomes proportional to $q^{-D}$ within the $q$ range $\xi^{-1} << q << a^{-1}$. For $q \leq 1/\xi$, $S'(q)$ exhibits a Guinier type behavior (Chaput et al., 1990). The radius of gyration of the aggregates $R_g$ is related with the correlation length by

$$R_g=[(D(D+1)/2]^{1/2}\xi.$$

Assuming that the primary particles are very small ($a << \xi$), the form factor of the monomer $P'(q)$ can be approximated by a constant function (Guinier, 1963)

$$P'(q) = v^2 \Delta\rho^2 \tag{4}$$

where $v$ is the monomer volume and $\Delta\rho$ the difference in scattering length density between monomer and matrix.

  

Taking into account equation (1) and that *P'(q)* is a constant, the scattering intensity produced by a concentrated set of aggregates *I(q)* can be expressed by

$$I(q) \propto S'(q)\, S(q), \tag{5}$$

where *S'(q)* is given by equation (3). As fractal aggregates are not centrosymmetric objects, the *S(q)* function should be understood as an effective structure function.

In dilute suspensions there is no spatial correlation between colloidal aggregates and so *S(q)* = 1 within the whole *q* range. In this case we simply have

$$I(q) = \phi\, P(q) \propto S'(q). \tag{6}$$

In concentrated suspensions, the fractal colloidal objects are closely located, inducing a more or less strong short-range order between them. Under this condition, the *S(q)* function oscillates around 1 and, consequently, the SAXS intensity exhibits characteristic interference peaks.

The function characterizing the short-range order for monoatomic real gases and liquid structures is the radial distribution function *G(r)*, defined by (Guinier, 1963):

$$G(r) = 4\pi r^2 p(r), \tag{7}$$

where *p(r)* is the pair correlation function. Assuming the average number of atoms per unit volume equal to *n*, *np(r)* is the average density number at a distance *r* from an atom located at the origin.

The same function *G(r)* defined by (7) can be used to characterize the short range order in isotropic systems of identical colloidal objects or aggregates embedded in a solvent.

The difference between the radial distribution function of the system and that corresponding to an ideal gas-like structure, $\Delta G = 4\pi r^2 [p(r)-1]$, can be determined by Fourier transform of the function $i(q) = S(q)-1$ (Guinier, 1963)

$$\Delta G(r) = (p(r)-1)4\pi r^2 = \frac{2r}{\pi}\int_0^\infty (S(q)-1)\sin(qr)\,dq, \tag{8}$$

where $\Delta G$ is the difference between (i) the average number of scattering objects in the studied system, located at a distance between *r* and *r+dr* from one of them, and (ii) the equivalent number for a homogeneous system without any short-range order.

## 3. Experimental

### 3.1. Sample preparation

The synthesis of $SnO_2$ aqueous colloidal suspensions has been described elsewhere (Hiratsuka, Pulcinelli & Santilli, 1990). Suspensions containing concentration of $SnO_2$ colloidal particles of 0.01, 0.03, 0.06, 0.08, 0.16, 0.33, 0.63 and 0.92 mol $L^{-1}$ were prepared by solvent dilution or evaporation of the 0.2 mol $L^{-1}$ suspension at 363 K under moderate magnetic stirring. To avoid destabilization and consequent gelation, the pH = 7.5 was kept constant by adding some drops of $NH_4OH$ aqueous solution during evaporation. The sol-gel transition was observed at room temperature for the most concentrated suspension ($[SnO_2]$ = 0.92 mol $L^{-1}$) in which the gel time is 80 min. In the suspensions with lower concentration, the sol-gel transition was not observed even several days after preparation.

### 3.2. SAXS measurements

The SAXS study was performed using the SAXS beamline of the National Synchrotron Light Laboratory (LNLS), Campinas, Brazil. This beamline is equipped with an asymmetrically cut and bent silicon (111) monochomator (λ = 1.608 Å) which yields a horizontally focused X-ray beam (Kellermann et al., 1997). A set of slits defines the beam vertically. A position sensitive X-ray detector and a multichannel analyzer were used to determine the SAXS intensity *I(q)* as function of the modulus of the scattering vector *q*. Because of the small size of the incident beam cross-section at the detection plane (less than 1 $mm^2$), no mathematical desmearing of the experimental function was needed.

Samples were put inside a cell between two thin films of Kapton separated by 0.5 mm. The SAXS intensity was determined as the difference between the total experimental scattering intensity produced by the suspension and that produced by the solvent (water). SAXS data were collected during 300 s for several suspensions with different concentration of $SnO_2$ particles. SAXS measurements of the most concentrated suspension ($[SnO_2]$ = 0.92 mol $L^{-1}$) were performed for different increasing periods of time. These *in situ* measurements were stopped when the sol-gel transition was completed.

## 4. Results and discussion

In order to determine the effective inter-aggregate structure function *S(q)* from the experimental *I(q)* ( $S(q) \propto I(q)/P(q)$, equation 1), the aggregate form factor, *P(q)*, have to be known. We determined *P(q)* for the different suspensions by fitting the *P(q)* theoretical function defined by (3) to the experimental *I(q)* functions. In the high q range interference effects are not significant, so *S(q)=1* and then $I(q) \propto P(q)$. In the low *q* range *S(q)* is expected to oscillate around 1. Therefore in the large *q* range the function *P(q)* (equation 3) was directly fitted to the experimental *I(q)* function and, over the low *q* range, the fitting parameters were chosen in such a way to maintain similar positive and negative deviations of *I(q)* with respect to *P(q)*.

The results of the fitting procedure for several suspensions containing different $SnO_2$ concentrations are shown in Fig. 1. Continuous lines correspond to the fitting of the theoretical function *P(q)* (given by (3)) to the experimental intensity curves following the procedure explained above.

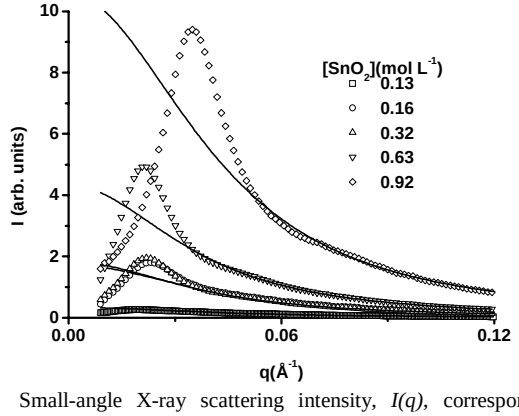


**Fig. 1:** Small-angle X-ray scattering intensity, *I(q)*, corresponding to colloidal suspensions with different $SnO_2$ concentration. Continuous lines represent fittings of the form factor function *P(q)* defined by (3).

The *P(q)* function defined by (3) fits well to the experimental intensity, measured in relative units, in the case of a dilute suspension ($[SnO_2]$ < 0.13 mol $L^{-1}$). This is an expected results because *S(q)=1*

over the whole $q$ range. This agreement confirms that the model assuming a fractal nature for the colloidal aggregates actually holds.

The value of the fractal dimension ($D$ = 2.3) and the size parameter of the primary particles ($a$ = 2.0 Å) are independent of sol concentration. The value $D$ = 2.3 is close to that expected for fractal aggregates formed by the mechanism of diffusion-limited aggregation ($D$ = 2.45) (Brinker & Scherrer, 1990). The correlation length of the fractal aggregates increases from 16 to 24 Å as the concentration increases from 0.08 to 0.16 mol $L^{-1}$. For concentrations above 0.16 mol $L^{-1}$ the correlation length of aggregates remains constant ($\xi$ = 24 Å) and a sharp peak is apparent at small $q$ in experimental SAXS curves. The height and sharpness of the scattering peaks increase with sol concentration while the maximum position remains almost constant up to [$SnO_2$] = 0.63 mol $L^{-1}$. For the highest concentration, [$SnO_2$] = 0.92 mol $L^{-1}$, the peak is shifted toward high $q$ values. This peak shifting in the *S(q)* function is classically expected for sols with increasing concentration (Belloni, 1986).

The effective inter-aggregate structure function, $S(q) \propto I(q)/P(q)$ (1) was determined for all concentrations from the results plotted in Fig. 1. The corresponding functions $i(q)=S(q)-1$ were plotted in Fig. 2. In the case of suspensions with low concentration, [$SnO_2$] = 0.13 mol $L^{-1}$, the *i(q)* function is close to zero for $q \geq 0.02$ $Å^{-1}$. A peak at $q \approx 0.025$ $Å^{-1}$ is apparent in the *i(q)* functions corresponding to suspensions with [$SnO_2$] ranging from 0.16 to 0.63 mol $L^{-1}$. As concentration increases from 0.16 to 0.63 mol $L^{-1}$ the peak height increases and the broadening is reduced. In the case of the most concentrated sol ([$SnO_2$] = 0.92 mol $L^{-1}$), the peak position in the *i(q)* function is clearly shifted toward high q range and a second maximum appears.

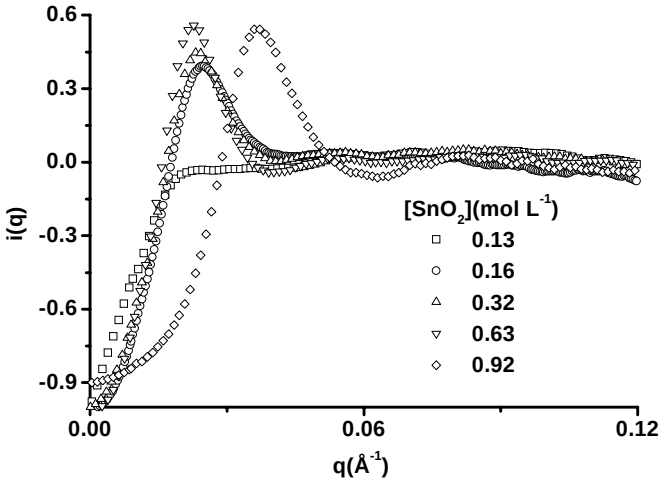


**Fig. 2:** *i(q)=S(q)-1* functions corresponding to colloidal suspensions with different $SnO_2$ concentrations.

Figure 3 shows the difference radial distribution function *ΔG(r)* calculated by Fourier transform of *i(q)* (8) corresponding to the suspensions with different concentrations. The curves corresponding to diluted suspensions ([$SnO_2$] ≤ 0.13 mol $L^{-1}$) do not show any remarkable oscillation, suggesting a weak, gas-like, short-range order of colloidal particles.

As concentration increases within the range from 0.13 up to 0.63 mol $L^{-1}$, the *ΔG(r)* function exhibits a large peak centred at 200 Å, analogous to that produced by concentrated real gases (Guinier, 1963). For concentrations from 0.16 up to 0.63 mol $L^{-1}$, the position of the maximum in *ΔG(r)*, corresponding to the most probable pair correlation distance between particles, remains approximately invariant. In this concentration range, the correlation length of the fractal aggregates ($\xi$ = 24 Å) also remains constant.

Two well-defined peaks are apparent in *ΔG(r)*, for the highest concentrated sol ([$SnO_2$] = 0.92 mol $L^{-1}$) revealing the existence of an incipient liquid-like short-range order between colloidal clusters. The average first and second-neighbor distances are $d_1$ = 125 Å and $d_2$ = 283 Å, respectively. The fractal correlation length of the primary aggregate is 20 Å. The existence of a liquid-like short-range order in the most concentrated suspension suggests that the colloidal clusters do not simply behave like a gas of non-interacting hard spheres and that electrostatic inter-particle interactions occur.

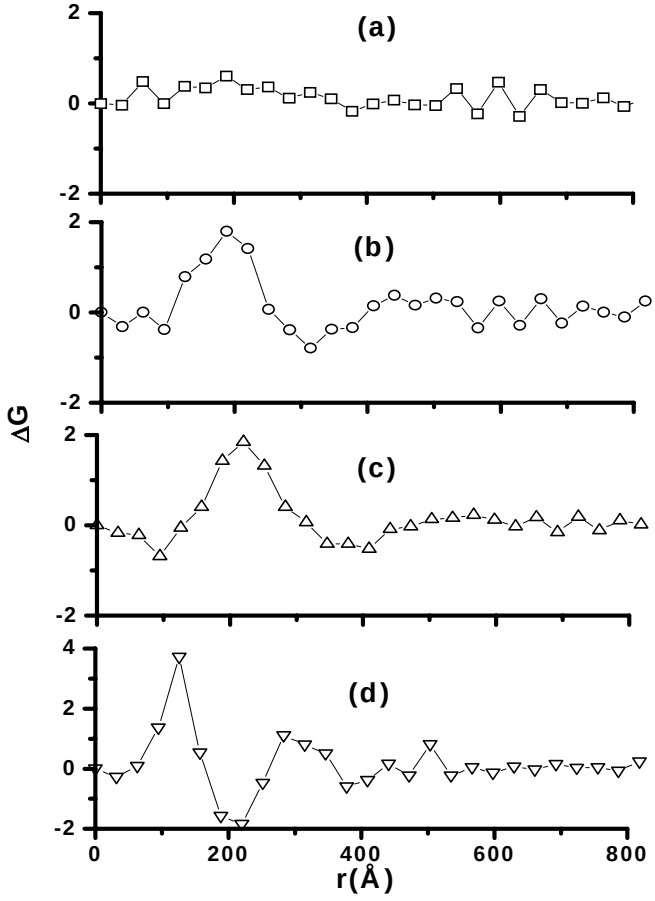


**Fig. 3:** Difference radial distribution function, *ΔG*, corresponding to sols with different concentrations: (a) 0.13, (b) 0.32, (c) 0.63 and (d) 0.92 mol $L^{-1}$.

The variations in SAXS intensity and *ΔG(r)* curves during the sol-gel transition ([$SnO_2$] = 0.92 mol $L^{-1}$) are shown in Fig. 4(a) and 4(b), respectively. The solid line (Fig. 4a) represents the best fitting of form factor $P(q) = S'(q)$, given by (3), to the experimental intensity for $q > 0.05$ $Å^{-1}$, keeping at lower $q$ values similar positive and negative deviations of *I(q)* with respect to *P(q)*. All SAXS curves, corresponding to different times, are similar. Both the phase and amplitude of oscillation of *ΔG(r)* (Fig. 4b), do not change appreciably with time. Consequently, the values of the adjustable parameters in (3) are approximately invariant ($D$ = 2.3, $a$ = 2 Å and $\xi$ = 20 Å). A small increase in the $r$-values corresponding to the second maximum of *ΔG(r)*, from 283 to 314 Å, and a noticeable decrease in the amplitude of the oscillation at larger distance ($r$ > 400 Å) are observed for time increasing from 1 to 85 min. This indicates a weak variation in the structure, which is less ordered after gelation.

We have observed that the studied sols are stable for low concentration and that only the most concentrated suspension transforms toward a gel, this transition being produced without any important structural change detected by SAXS. This behavior suggests that gelation is promoted by the formation of a few connections between the colloidal fractal clusters embedded in the solvent. This implies that the gel network has a tenuous structure as previously suggested by measurements of rheological properties (Santos, Santilli & Pulcinelli, 1998).

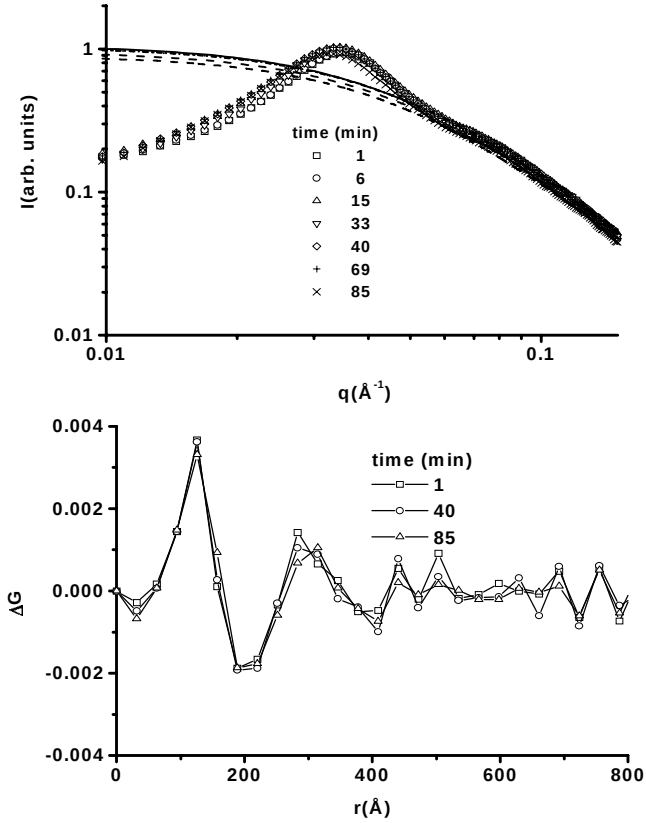


**Fig. 4:** (a) Log-log plots of the small-angle X-ray scattering intensity as functions of the wave number $q$ for [$SnO_2$] = 0.92mol $L^{-1}$ for different gelation times. The continuous lines represent fittings of the $P(q)$ function defined by (3). (b) Evolution of $\Delta G$ function during the sol-gel transition.

Figure 5 shows a model of the colloidal primary aggregates, their short-range order and a schematic description of the sol-gel transition. Diluted $SnO_2$ sols with concentrations ranging from 0.01 up to 0.16 mol $L^{-1}$ are constituted by fractal clusters, formed by aggregation of small primary units ($a \cong 2$ Å), with a size characterised by a correlation lengths ranging from 16 to 24 Å. For concentrations smaller than 0.13 mol $L^{-1}$ no peaks in the structure function was observed, so the inter-aggregate distances are large and the fraction of excluded volume is small. These systems can be described as an "ideal gas" of colloidal particles. As concentration increases from 0.16 up to 0.64 mol $L^{-1}$, the correlation length of fractal clusters and the average distance between them remains constant ($\xi$ = 24 Å and $d_1$ = 200 Å) and a certain degree of interaction between neighbour fractal clusters occurs. In this concentration range the colloidal aggregates are arranged as a real gas. The correlation length of the aggregates corresponding to the highest sol concentration (0.92 mol $L^{-1}$) is significantly smaller than that of aggregates in diluted suspensions ($\xi$ = 18 Å for 0.92 mol $L^{-1}$ and $\xi$ = 24 Å for 0.64 mol $L^{-1}$). The reduction in correlation length for increasing concentration is probably a consequence of the decrease in the average distances between aggregates which induces their interpenetration. This would promote modifications and/or rupture of peripheric branches of the fractal structure. On the other hand, the shape of the $\Delta G$ function suggests that concentrated sols exhibit a fluid-like structure

The differential radial distribution function does not appreciably change during the sol-gel transition indicating that the neighbour average distances between aggregates and the coordination numbers remain invariant. This result supports the conclusion of a previous investigation of rheological properties of suspensions (Santos, Pulcinelli & Santilli, 1998) suggesting that secondary aggregation of fractal colloidal objects proceeds by one dimensional growth, so producing in gel state a network constituted essentially by linear chains.

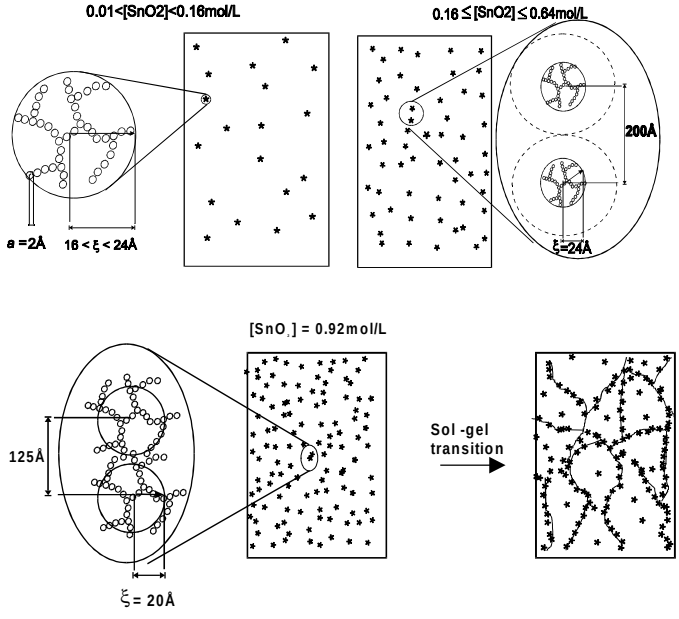


**Fig. 5:** Schematic model for the structure of suspensions with different $SnO_2$ concentrations.

## 5. Conclusion

This SAXS study allowed us to establish the basic structural features of colloidal $SnO_2$ particles embedded in aqueous suspensions under different concentration conditions.

i) Stable diluted sols are composed of colloidal aggregates with a fractal structure forming an ideal gas-like arrangement. The correlation length that characterises the size of the fractal aggregates increases for increasing sol concentration.

ii) Stable sols with intermediate concentrations exhibit a real gas-like arrangement. The size of the aggregates and the average distance between them are independent of concentration.

iii) Highly concentrated sols exhibit a fluid-like structure consisting of more closely arranged aggregates with a comparatively small fractal correlation length.

iv) The structure of the fractal aggregates is essentially invariant during the sol-gel transition. The presented results support the conclusion of a previous investigation suggesting that secondary aggregation of fractal clusters during the sol-gel transition is an essentially linear process leading to a network constituted by linear chains.

The fitting of theoretical models for interaction between colloidal particles to the experimental structure functions determined in the present study is an open question for future investigation.

This work was partially performed at LNLS/Brazil. Financial support from FAPESP and PRONEX/MCT (Brazilian funding agencies) and COFECUB (France/Brazil) is acknowledged.

**References**

Alami-Younssi, S., Larbot, A., Persin, M., Sarrazin, J. & Cot, L. (1994). *J. Mem. Sci.* **91,** 87-93.

Belloni, L. (1986). *J. Chem. Phys.* (1) **85**, 519-523.

Brinker, C.J. & Scherer, G.W. (1990). *Sol-Gel Science*, Chap. 13 and 14. San Diego: Academic Press.

Briois, V., Santilli, C.V., Pulcinelli, S.H. & Brito, G.E.S. (1995). *J. Non-Cryst. Solids* **191**, 17-28.

Brito, G.E.S., Pulcinelli, S.H. & Santilli C.V. (1994). *J. Sol-Gel Sci. and Tech.* **2**, 575-562.

Chaput, F., Boilot, J.P., Dauger, A., De Vreux, F. & De Geyer, A. (1990). *J. Non-Cryst. Solids* **116,** 133-139.

Chiavacci, L.A., Santilli, C.V., Pulcinelli S.H. & Craievich, A. F. (1997). *J. Appl. Cryst*. **30,** 750-754.

Cot, L. (1991). *J. Chim. Phys.* **88,** 2083-2091.

Guinier, A. (1963*). X- Ray Diffraction in Crystals, Imperfect Crystals and Amorphous Bodies*. San Francisco: W.H. Freeman and Company.

Hiratsuka, R.S., Pulcinelli, S.H. & Santilli, C.V. (1990). *J. Non-Cryst. Solids* **121,** 76-83.

Kellermann, G., Vicentin, F., Tamura, E., Rocha, M., Tolentino, H. Barbosa, A. F., Craievich, A. F. & Torriani, I. L. (1997). *J. Appl. Cryst*. **30**, 880-883.

Santilli, C.V., Pulcinelli, S.H. & Craievich, A. F. (1995). *Phys Rev B* **51,** 8801-8809.

Santos, L.R.B., Larbot, A., Santilli, C.V. & Pulcinelli, S.H. (1998). J. Sol-Gel Sci. Tech. **13,** 805-811.

Santos, L.R.B., Pulcinelli, S.H. & Santilli, C.V. (1997). *J. Sol-Gel Sci. and Tech.*, **8,** 477-481.

Santos, L.R.B., Santilli, C.V, & Pulcinelli, S.H., (1998) *J. Non-Cryst. Solids* **247,** 153-157 .

Teixeira, J. (1988). *J. Appl. Cryst.* **21,** 781-785.

Vollet, D.R., Hiratsuka, R.S., Pulcinelli, S.H., Santilli, C.V. & Craievich, A.F. (1992). *J. Non-Cryst. Solids* **142,** 181-184.